



Nonstandard continualization of 1D lattice with next-nearest interactions. Low order ODEs and enhanced prediction of the dispersive behavior

F. Gómez-Silva , J. Fernández-Sáez & R. Zaera

To cite this article: F. Gómez-Silva , J. Fernández-Sáez & R. Zaera (2020): Nonstandard continualization of 1D lattice with next-nearest interactions. Low order ODEs and enhanced prediction of the dispersive behavior, Mechanics of Advanced Materials and Structures, DOI: [10.1080/15376494.2020.1799271](https://doi.org/10.1080/15376494.2020.1799271)

To link to this article: <https://doi.org/10.1080/15376494.2020.1799271>



© 2020 The Author(s). Published with license by Taylor and Francis Group, LLC



Published online: 07 Aug 2020.



Submit your article to this journal [↗](#)



Article views: 94



View related articles [↗](#)



View Crossmark data [↗](#)

Nonstandard continualization of 1D lattice with next-nearest interactions. Low order ODEs and enhanced prediction of the dispersive behavior

F. Gómez-Silva, J. Fernández-Sáez, and R. Zaera

Department of Continuum Mechanics and Structural Analysis, University Carlos III of Madrid, Avda. de la Universidad, Leganés, Madrid, Spain

ABSTRACT

In this article, different standard and nonstandard continualization techniques are applied to a one-dimensional solid consisting in a chain of masses interacting with nearest and next-nearest neighbors through linear springs. The study focuses on the reliability of the different continua in capturing the dispersive behavior of the discrete, on the order of the continuous governing equation because of its effect on the need for including nonclassical boundary conditions, as well as on the physical inconsistencies that appear for short wavelengths. The Regularization method, used by Bacigalupo and Gambarotta for a lattice with nearest interactions, presents advantages over the others.

ARTICLE HISTORY

Received 9 June 2020
Accepted 18 July 2020

KEYWORDS

Next-nearest interactions; lattice dynamics; dispersive behavior; continualization; shift operator; regularization

1. Introduction



Formulations based on classical continuum mechanics fail when applied to problems in which size effects are present due to the discreteness of the matter. To deal with this kind of problem, lattice dynamic and molecular dynamics approaches appear as an alternative to classical continuum models. Nevertheless, these frameworks require a very high computational cost. Therefore, a considerable effort is devoted to develop nonclassical continuum models that could be able to reproduce the intrinsic dispersive behavior of the discrete media. Although the first attempts to capture the effects of microstructure using the higher-order equations of elasticity could be dated in the nineteenth century (works by Cauchy and Voigt), and in the beginning of the twentieth century (works by Cosserat brothers), these approaches experienced a great revival in the 1960s and 1970s with the works by Mindlin, Toupin, or Eringen, among others. The interest in these approaches remains to this day with works like Tadi Beni et al. [1], Shafiei et al. [2], and Barretta et al. [3]. These theories can be considered axiomatic frameworks that need new equilibrium equations to govern the higher-order stresses, as well as a large number of new nonclassical constants, that have to be calibrated from experimental results. However, an alternative to the axiomatic approaches is that based on the *continualization* of the discrete system, trying to relate the new parameters with geometrical and mechanical characteristics of the lattice.

The Born-Von Kármán lattice composed by a one-dimensional (1D) chain of identical masses connected with linear

springs (i.e. nearest neighbor interaction), is the simplest lattice model to understand the dispersive behavior of discrete media. It has been widely studied and it is possible to show that this model leads to the classical linear elastic rod equation when a standard (based on Taylor expansions) continualization of low order is applied to the discrete displacement field. Polyzos and Fotiadis [4] showed different continualization procedures, leading to different continuous governing equations, all of them with fourth-order spatial derivatives. Considering the linear spring with distributed mass, and developing a standard continualization of the total energy of the system [4], it is possible to recover the governing equation of a rod modeled with Form-II of the strain gradient elasticity of Mindlin [5].

Nonstandard continualization techniques have been also used [6–9]. These techniques consist in transforming the discrete equations into pseudodifferential equations, which are later expanded by Taylor series [6, 7, 9] or by Padé approximants [8]. Bacigalupo and Gambarotta [7] proposed an enhanced continualization scheme in which, besides using pseudodifferential operators, a central difference scheme is employed to discretize the first spatial derivative of the continuous displacement, achieving a continuous governing equation of higher order than that corresponding to the classical one. This approach has been applied to several 1D systems: a rod lattice, a beam lattice with node rotations, and a beam lattice with generalized displacements [7].

In the context of 1D nonlinear lattices, Vila et al. [10] proposed a nonstandard continualization of a kind of nonlinear system, defined as a discrete chain of masses interacting through nonlinear springs, analogous to the Fermi-Pasta-Ulam-Tsingou

CONTACT F. Gómez-Silva  frgomez@ing.uc3m.es  Department of Continuum Mechanics and Structural Analysis, University Carlos III of Madrid, Avda. de la Universidad, Leganés, Madrid, Spain.

This article has been republished with minor changes. These changes do not impact the academic content of the article.

© 2020 The Author(s). Published with license by Taylor and Francis Group, LLC

This is an Open Access article distributed under the terms of the Creative Commons Attribution-NonCommercial-NoDerivatives License (<http://creativecommons.org/licenses/by-nc-nd/4.0/>), which permits non-commercial re-use, distribution, and reproduction in any medium, provided the original work is properly cited, and is not altered, transformed, or built upon in any way.

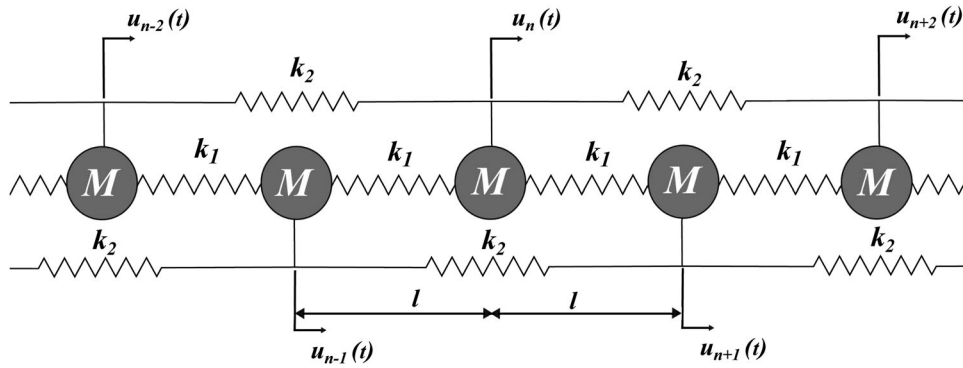


Figure 1. Nearest and next-nearest interaction lattice model.

system [11]. The results obtained by this nonstandard method reproduce the dynamic behavior of the lattice more accurately than those corresponding to the nonlinear classical continuum.

One-dimensional lattices with springs connecting nearest neighbors as well as next-nearest neighbors are also extensively studied. Most works analyze the discrete model, either considering it as a finite (bounded) solid and analyzing the effect of the number of masses that form the system [12–15], or as an infinite solid, studying their dispersion relations [16, 17]. Triantafyllidis and Bardenhagen [18] and Metrikine [19] proposed a nearest and next-nearest interactions system and compared it with high-order gradient theories. On the other hand, Di Paola et al. [20] and Zingales [21] studied nonlocal elastic models and used this discrete system to show their mechanical equivalence. Fewer works apply continualization techniques to this kind of system with nearest and next-nearest interactions. Polyzos and Fotiadis [4] and Tarasov [22] employed standard continualization methods to achieve a continuous governing equation which allows to capture the behavior of the discrete system.

In general, work centered on the development (using both continuum techniques and axiomatic theories) of continuous models to capture the size effects present in discrete media, focuses on an adequate representation of their dispersive behavior. For this purpose, high order governing equations are commonly used to approximate the dispersion relation toward the high wavelength zone. For the study of wave propagation phenomena in unbounded solids, the use of high order governing equations may not pose a major problem. However, these equations require nonclassical boundary conditions, the physical interpretation of which is not simple, for their resolution when considering finite solids. In this sense, the proposal of low order models that maintain a precise approximation of the dispersion ratio in a wide range of wavelengths is of interest for real applications in the microscale and nanoscale. In addition, the use of continualization techniques allows to establish the relationship between the parameters of discrete and continuous models, thus avoiding calibration.

In this article, the analysis of a 1D linear lattice with nearest and next-nearest neighbor interactions is revisited. Different continualization techniques are used and, for the first time, some nonstandard methods of continualization are applied to this kind of system with next-nearest springs. The dispersion relations obtained with the different continualized equations are compared with those derived from the

discrete system, with the regularization procedure proposed by Bacigalupo and Gambarotta [7] applied to a nearest and next-nearest lattice for the first time here, showing the best performance. Interestingly, this model leads to continuous equations with second-order derivatives in the spatial variable. Therefore, nonclassical boundary conditions are not needed to solve the dynamics of a finite system.

There are a number of engineering problems in which the characteristic length of the phenomena studied is similar to the size of the microstructure. A clear example of this is the nanostructures used in engineering applications such as nanoelectromechanical and microelectromechanical sensors [23], which are widely used in robotics and biosensors [24, 25]. Similarly, size effects can also appear in structures at the meso or macroscale, like in composites and polycrystalline solids and granular materials. On the other hand, in the last years, wave propagation phenomena in metamaterials has generated a great interest [26–28] because of the ability of these materials to manipulate and control waves, thanks to the unconventional properties inherited from their lattice structure. Hence, the need for continuum mechanics theories that permit to account for scale effects [29, 30].

The article is organized as follows. In Section 2, the discrete model, taken as a reference, is introduced. Its discrete governing equation is achieved, and its dispersion relation and phase velocity are presented. In Section 3, the different continualization procedures are described and the dispersion relations of the different models are obtained. In Section 4, all models are compared, highlighting their advantages and drawbacks. Finally, in Section 5, some concluding remarks are presented.

2. Discrete reference model

In this section, the discrete system, considered here as a reference, is introduced. This model is made up of a chain formed by a number of N identical particles with mass M , interacting with each other through linear springs. These particles are equally spaced at distance l , which is considered as a characteristic length, so the chain length is defined by $L = l(N - 1)$, and the reference position of an arbitrary particle n is $x_n = (n - 1)l$, $n = 1, \dots, N$. As can be observed in Figure 1, springs which connect nearest particles have stiffness k_1 and those that join next-nearest particles have stiffness k_2 . It is well known that the interaction force between

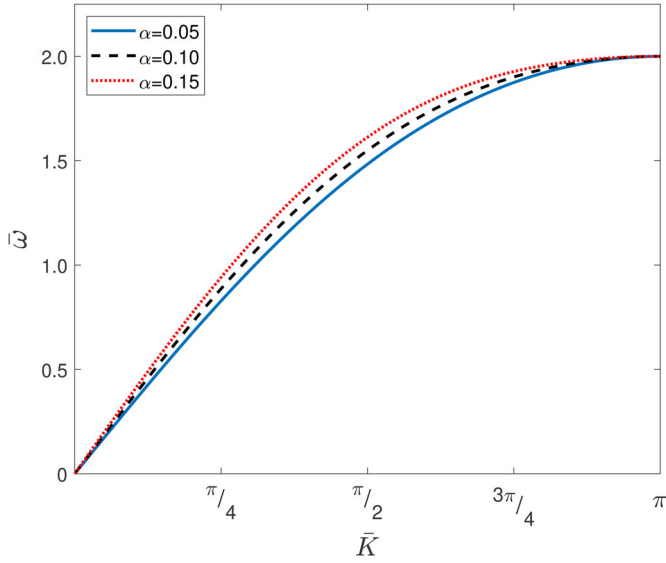


Figure 2. Dispersion curves of the discrete model for different values of α .

particles decays with the distance, so that it can be assumed that the value of k_1 is significantly higher than that of k_2 . The displacement variables are defined as $u_n(t)$, $n = 1, \dots, N$, where t is the time variable.

Keeping in mind the previous considerations, the dimensionless governing equations of the system can be obtained as follows, using the following parameters and variables

$$\begin{aligned} \bar{u}_n &= \frac{u_n}{l}; & \bar{x}_n &= \frac{x_n}{l}; & \bar{t} &= \tilde{\omega}t; & \tilde{\omega} &= \sqrt{\frac{k_1}{M}}; \\ \alpha &= \frac{k_2}{k_1}; & \bar{W} &= \frac{W}{k_1 l^2}; & \bar{T} &= \frac{T}{k_1 l^2}; \end{aligned} \quad (1)$$

where W and T are the potential and kinetic energy, respectively. The dimensionless potential energy of the linear elastic lattice is defined by

$$\bar{W} = \sum_{n=1}^{N-1} \frac{1}{2} (\bar{u}_{n+1} - \bar{u}_n)^2 + \sum_{n=1}^{N-2} \frac{1}{2} \alpha (\bar{u}_{n+2} - \bar{u}_n)^2, \quad (2)$$

and the dimensionless kinetic energy of the system is

$$\bar{T} = \sum_{n=1}^N \frac{1}{2} (\partial_{\bar{t}} \bar{u}_n)^2, \quad (3)$$

where $\partial_{\bar{t}}$ refers to the dimensionless time derivative. The dimensionless Lagrangian of the system is

$$\bar{\mathcal{L}} = \bar{T} - \bar{W}, \quad (4)$$

where $\bar{\mathcal{L}} = \mathcal{L}/(k_1 l^2)$ and \mathcal{L} is its dimensional counterpart.

Through the use of Lagrange equations, the dimensionless governing equation for an interior particle n is obtained

$$\partial_{\bar{t}\bar{t}} \bar{u}_n = (\bar{u}_{n+1} + \bar{u}_{n-1} - 2\bar{u}_n) + \alpha(\bar{u}_{n+2} + \bar{u}_{n-2} - 2\bar{u}_n). \quad (5)$$

Now, the dispersive behavior of the model is studied. For this purpose, we assume that Eq. (5) admits a plane wave solution of the form

$$\bar{u}_n = \bar{u}_0 e^{i(\bar{K}\bar{x}_n - \bar{\omega}\bar{t})}, \quad (6)$$

where $\bar{K} = Kl$ is the wavenumber and $\bar{\omega} = \omega/\tilde{\omega}$ the wave frequency, both dimensionless, being K and ω their

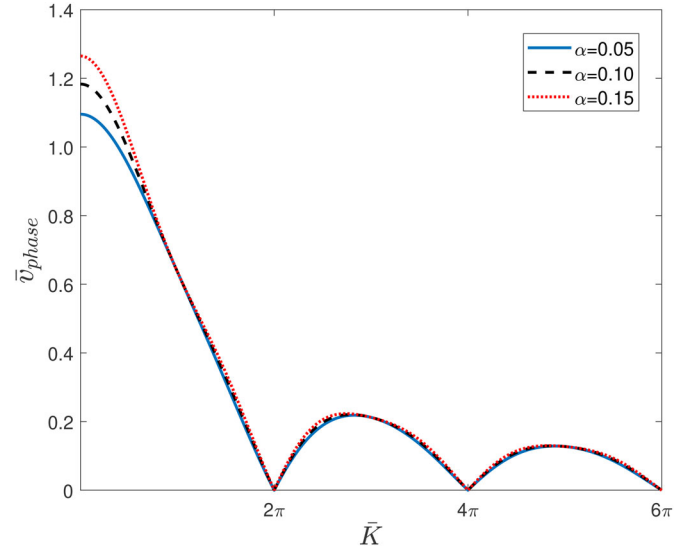


Figure 3. Phase velocity of the discrete model for different values of α .

dimensional counterparts. From Eqs. (5) and (6), the dispersion equation, relating the wavenumber and the frequency, can be found

$$\bar{\omega} = \sqrt{2(1 - \cos(\bar{K})) + 2\alpha(1 - \cos(2\bar{K}))}. \quad (7)$$

This dispersion relation is nonlinear, and depends on the dimensionless parameter α , which relates the springs stiffness. In Figure 2, dispersion curves of the discrete model, for the irreducible Brillouin zone $\bar{K} \in [0, \pi]$ [31], are shown. These curves correspond to different values of α . Since k_1 is considerably greater than k_2 , $\alpha = 0.15$ is considered here to be the upper limit for a practical case. It can also be seen how a Band Gap appears. This kind of behavior can be contrasted with experimental results such as those presented by Eringen [32].

Another possibility to study the system's dispersive behavior is analyzing its phase velocity, which is calculated as

$$\bar{v}_{\text{phase}} = \frac{\bar{\omega}}{\bar{K}} = \frac{\sqrt{2(1 - \cos(\bar{K})) + 2\alpha(1 - \cos(2\bar{K}))}}{\bar{K}}. \quad (8)$$

Figure 3 shows the phase velocity related to the model, for different values of α . As can be observed in Figures 2 and 3, the role of the parameter α is to increase the system's stiffness.

3. Different continualization methods

As verified in the previous section, the discrete model shows dispersive behavior. In order to achieve continuous equations capturing this behavior, different methods of continualization applied to the discrete system are studied. The first group includes those using standard techniques, where Taylor's series are employed to expand the displacement variables. The rest of the methods are based on nonstandard techniques, using pseudodifferential operators.

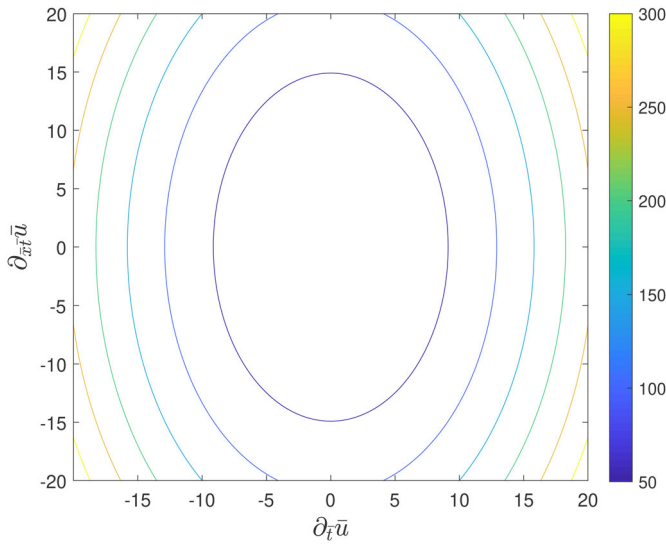


Figure 4. Nonclassical potential energy corresponding to the Standard II model. Isoenergy curves for $\alpha = 0.05$.

3.1. Standard continualization

To obtain an equivalent continuous model, one of the simplest continualization procedures consists in expanding the displacements variables by Taylor series as

$$\begin{aligned} \bar{u}_{n\pm m} &= \bar{u}(\bar{x}, \bar{t}) \pm \frac{\partial \bar{u}(\bar{x}, \bar{t})}{\partial \bar{x}} m\bar{l} + \frac{1}{2} \frac{\partial^2 \bar{u}(\bar{x}, \bar{t})}{\partial \bar{x}^2} (m\bar{l})^2 \\ &\pm \frac{1}{6} \frac{\partial^3 \bar{u}(\bar{x}, \bar{t})}{\partial \bar{x}^3} (m\bar{l})^3 \\ &+ \frac{1}{24} \frac{\partial^4 \bar{u}(\bar{x}, \bar{t})}{\partial \bar{x}^4} (m\bar{l})^4 \pm O\left(\frac{\partial^5}{\partial \bar{x}^5}\right); \quad m = 1, 2, \end{aligned} \quad (9)$$

where $\bar{u}(\bar{x}, \bar{t})$ is the continuous displacement such that $\bar{u}_n(\bar{t}) = \bar{u}(\bar{x}_n, \bar{t})$ and $\bar{l} = l/l = 1$. Equation (9) is written with dimensionless variables. Therefore, the approximation order is determined by the order of the spatial dimensionless derivative.

In this section, two different standard continualization methods are employed, expanding either the discrete governing Eq. (5), or the Lagrangian of the system. These models, for the remainder of this document, will be mentioned as Standard I and Standard II models, respectively.

3.1.1. Standard I model

If expression (9) is introduced in the discrete dimensionless governing Eq. (5), including terms up to second order, it turns into the governing equation

$$a_1 \partial_{\bar{x}\bar{x}} \bar{u} = \partial_{\bar{t}\bar{t}} \bar{u}, \quad (10)$$

where $\partial_{\bar{x}}$ refers to the dimensionless position derivative and

$$a_1 = 1 + 4\alpha. \quad (11)$$

As can be seen, Eq. (10) is similar to the simple classical rod equation, adding the parameter α , which increases the stiffness of the continuous model. Assuming a plane wave solution

$$\bar{u} = \bar{u}_0 e^{i(\bar{K}\bar{x} - \bar{\omega}\bar{t})}, \quad (12)$$

the dispersion relation of this continuous model is

$$\bar{\omega} = \sqrt{a_1} \bar{K}. \quad (13)$$

This equation satisfactorily describes long wave propagation ($\bar{K} \rightarrow 0$) in the discrete system. Nevertheless, this does not occur for short waves, whose propagation is affected by the solid's microstructure. To account for dispersive behavior, it is necessary to keep terms until fourth order in Eq. (9). In this way, now Eq. (5) takes the form

$$a_1 \partial_{\bar{x}\bar{x}} \bar{u} - a_2 \partial_{\bar{x}\bar{x}\bar{x}\bar{x}} \bar{u} = \partial_{\bar{t}\bar{t}} \bar{u}, \quad (14)$$

where

$$a_1 = 1 + 4\alpha; \quad a_2 = -\frac{1}{12}(1 + 16\alpha). \quad (15)$$

As can be noted, by means of including fourth-order derivatives, an internal scale factor, a_2 , is introduced. The dispersion relation in this case is

$$\bar{\omega} = \bar{K} \sqrt{a_1 + a_2 \bar{K}^2}, \quad (16)$$

which predicts a dispersive behavior.

3.1.2. Standard II model

Following a different approach, Polyzos and Fotiadis [4] expanded the discrete displacements in the potential energy expression. The expression of the dimensionless potential energy is written as

$$\begin{aligned} \bar{W}_l &= \frac{1}{2} \left\{ \frac{1}{2} [\bar{u}_n - \bar{u}_{n-1}]^2 + \frac{1}{2} [\bar{u}_{n+1} - \bar{u}_n]^2 \right\} \\ &+ \frac{1}{2} \left\{ \frac{1}{2} \alpha [\bar{u}_n - \bar{u}_{n-2}]^2 + \frac{1}{2} \alpha [\bar{u}_{n+2} - \bar{u}_n]^2 \right\}. \end{aligned} \quad (17)$$

Equation (17) can be expanded via Taylor's series with Eq. (9), until second order in this case, leading to

$$\bar{W}_l = \frac{1}{2} \left[(\partial_{\bar{x}} \bar{u})^2 + \frac{1}{4} (\partial_{\bar{x}\bar{x}} \bar{u})^2 \right] + \frac{\alpha}{2} \left[4(\partial_{\bar{x}} \bar{u})^2 + 4(\partial_{\bar{x}\bar{x}} \bar{u})^2 \right], \quad (18)$$

which is positive definite regardless of the value of α , as can be easily proven. Figure 4 shows isoenergy curves of Eq. (18) and its functional dependence on strain and strain gradient.

The dimensionless kinetic energy is written as

$$\bar{T}_l = \frac{1}{2} (\partial_{\bar{t}} \bar{u})^2. \quad (19)$$

The dimensionless Lagrangian of this model becomes

$$\begin{aligned} \bar{\mathcal{L}}_l &= \frac{1}{2} (\partial_{\bar{t}} \bar{u})^2 - \frac{1}{2} \left[(\partial_{\bar{x}} \bar{u})^2 + \frac{1}{4} (\partial_{\bar{x}\bar{x}} \bar{u})^2 \right] \\ &- \frac{\alpha}{2} \left[4(\partial_{\bar{x}} \bar{u})^2 + 4(\partial_{\bar{x}\bar{x}} \bar{u})^2 \right]. \end{aligned} \quad (20)$$

All the above energy variables have been calculated per unit length and are written in dimensionless form dividing by $k_1 l$.

Applying the Hamilton's Principle to the Eq. (20), the following governing equation is obtained

$$a_1 \partial_{\bar{x}\bar{x}} \bar{u} - a_2 \partial_{\bar{x}\bar{x}\bar{x}\bar{x}} \bar{u} = \partial_{\bar{t}\bar{t}} \bar{u}, \quad (21)$$

where

$$a_1 = 1 + 4\alpha; \quad a_2 = \frac{1}{4}(1 + 16\alpha). \quad (22)$$

The structures of Eqs. (14) and (21) are identical, and the only difference is the value of a_2 , which leads to different dispersive behaviors. In this case, the dispersion equation is also given by Eq. (16). An interesting discussion about this continualization technique can be found in [33] and [34].

Both Eqs. (14) and (21) include fourth order spatial derivatives. This implies that in problems involving finite (bounded) solids, it is necessary to impose four boundary conditions to solve it, two of them being nonclassical, whose physical meaning is unclear.

3.2. Nonstandard continualization via shift operator

In this section, nonstandard continualization methods are used, applying the shift operator [10]

$$\bar{u}_{n\pm m} = \bar{E}^{\pm m} \bar{u}_n; \quad m = 1, 2. \quad (23)$$

where

$$\bar{E} = e^{\bar{j}\partial_{\bar{x}}}, \quad (24)$$

First, the shift operator will be applied to the discrete governing Eq. (5), using Padé approximants, as Kevrekidis et al. [8] proposed for a nearest interaction lattice. On the other hand, the shift operator will also be applied to the kinetic energy of the system in order to obtain a nonclassical enriched kinetic energy (EKE; see [9] and [35]). Lastly, the Regularization method, proposed by Bacigalupo and Gambarotta [7] for nearest interactions model, is applied. These three models, for the rest of this document, will be referred as Padé, EKE, and Regularization, respectively.

3.2.1. Padé model

Substituting Eq. (23) in the discrete governing Eq. (5), results

$$\partial_{\bar{t}\bar{t}} \bar{u}_n = [(e^{\partial_{\bar{x}}} + e^{-\partial_{\bar{x}}} - 2) + \alpha(e^{2\partial_{\bar{x}}} + e^{-2\partial_{\bar{x}}} - 2)] \bar{u}_n, \quad (25)$$

and taking into account trigonometric identities, we get

$$\partial_{\bar{t}\bar{t}} \bar{u}_n = \left[4\sinh\left(\frac{\partial_{\bar{x}}}{2}\right) + 4\alpha\sinh(\partial_{\bar{x}}) \right] \bar{u}_n. \quad (26)$$

Now, the pseudodifferential operators are expressed via Padé (2,2) approximants

$$4\sinh\left(\frac{\partial_{\bar{x}}}{2}\right) \approx \frac{\partial_{\bar{x}}^2}{1 - \frac{1}{12}\partial_{\bar{x}}^2}, \quad (27)$$

$$4\sinh(\partial_{\bar{x}}) \approx \frac{4\partial_{\bar{x}}^2}{1 - \frac{1}{3}\partial_{\bar{x}}^2}. \quad (28)$$

Considering that $\bar{u}_n = \bar{u}(\bar{x}, \bar{t})$, and Eqs. (27) and (28), the following continuous governing equation is obtained

$$\begin{aligned} & (1 + 4\alpha)\partial_{\bar{x}\bar{x}}\bar{u} - \frac{1}{3}(1 + \alpha)\partial_{\bar{x}\bar{x}\bar{x}\bar{x}}\bar{u} \\ & = \partial_{\bar{t}\bar{t}}\bar{u} - \frac{5}{15}\partial_{\bar{x}\bar{x}\bar{t}\bar{t}}\bar{u} + \frac{1}{36}\partial_{\bar{x}\bar{x}\bar{x}\bar{t}\bar{t}}\bar{u}, \end{aligned} \quad (29)$$

Keeping terms including factors up to \bar{l}^3 in dimensional form (see Appendix), we get the continuous governing equation of this model

$$a_1\partial_{\bar{x}\bar{x}}\bar{u} - a_2\partial_{\bar{x}\bar{x}\bar{x}\bar{x}}\bar{u} = \partial_{\bar{t}\bar{t}}\bar{u} - a_3\partial_{\bar{x}\bar{x}\bar{t}\bar{t}}\bar{u}, \quad (30)$$

where

$$a_1 = 1 + 4\alpha; \quad a_2 = \frac{1}{3}(1 + \alpha); \quad a_3 = \frac{5}{12}. \quad (31)$$

In this case, a new scale parameter a_3 appears, which increases the flexibility of the model, according to the dispersion relation equation

$$\bar{\omega} = \bar{K} \sqrt{\frac{a_1 + a_2\bar{K}^2}{1 + a_3\bar{K}^2}}. \quad (32)$$

As can be observed, the Eq. (30) includes a fourth-order spatial derivative, which implies the use of nonclassical boundary conditions. This does not occur when this method is applied to a nearest interaction lattice, where fourth-order spatial derivatives do not appear [8]. In order to achieve a continuous governing equation without fourth-order spatial derivatives, in the case of nearest and next-nearest interactions, the following novel nonstandard continualization method is proposed.

3.2.2. EKE model

A different continualization method consists in extending the displacements in the Lagrangian of the system, in a similar way to the Standard II model. In this case, the potential energy density per unit of length is extended via Taylor's series until first order (classical potential energy)

$$\bar{W}_l = (1 + 4\alpha)(\partial_{\bar{x}}\bar{u})^2. \quad (33)$$

On the other hand, to succeed in capturing the dispersive behavior, the kinetic energy can be considered in a nonclassical way. Rosenau [9] suggests a nonstandard expression of the kinetic energy of the discrete system

$$\bar{T}_l = \frac{1}{2} \left((\partial_{\bar{t}}\bar{u})^2 + \frac{1}{12}(\partial_{\bar{x}\bar{t}}\bar{u})^2 \right). \quad (34)$$

Applying Hamilton's Principle to the new Lagrangian expression

$$\bar{\mathcal{L}}_l = \frac{1}{2} \left((\partial_{\bar{t}}\bar{u})^2 + \frac{1}{12}(\partial_{\bar{x}\bar{t}}\bar{u})^2 \right) - (1 + 4\alpha)(\partial_{\bar{x}}\bar{u})^2, \quad (35)$$

the governing equation obtained is

$$a_1\partial_{\bar{x}\bar{x}}\bar{u} = \partial_{\bar{t}\bar{t}}\bar{u} - a_3\partial_{\bar{x}\bar{x}\bar{t}\bar{t}}\bar{u}, \quad (36)$$

where

$$a_1 = 1 + 4\alpha; \quad a_3 = \frac{1}{12}. \quad (37)$$

The corresponding dispersion equation is

$$\bar{\omega} = \bar{K} \sqrt{\frac{a_1}{1 + a_3\bar{K}^2}}, \quad (38)$$

which is nonlinear and depends on the dimensionless parameter α . In this case, the scale parameter a_3 appears again, now with a value $a_3 = 1/12$.

Table 1. Values of the parameters for the continuous models.

	a_1	a_2	a_3
Classic	$1 + 4\alpha$	0	0
Standard I	$1 + 4\alpha$	$-\frac{1}{12}(1 + 16\alpha)$	0
Standard II	$1 + 4\alpha$	$\frac{1}{4}(1 + 16\alpha)$	0
Padé	$1 + 4\alpha$	$\frac{1}{3}(1 + \alpha)$	5/12
EKE	$1 + 4\alpha$	0	1/12
Regularization	$1 + 4\alpha$	0	1/6

3.2.3. Regularization model

Another continualization method, proposed by Bacigalupo and Gambarotta [7], is here considered. Using the central difference scheme for the first derivative of the continuous displacement

$$\left. \frac{\partial \bar{u}}{\partial \bar{x}} \right|_{x_n} = \frac{\bar{u}_{n+1} - \bar{u}_{n-1}}{2}, \quad (39)$$

and applying the shift operator

$$\left. \frac{\partial \bar{u}}{\partial \bar{x}} \right|_{x_n} = \partial_{\bar{x}} \bar{u} \Big|_{x_n} = \frac{e^{\partial_{\bar{x}}} - e^{-\partial_{\bar{x}}}}{2} \bar{u}_n, \quad (40)$$

an expression relating discrete and continuous fields is obtained

$$\bar{u}_n = \frac{2\partial_{\bar{x}}}{e^{\partial_{\bar{x}}} - e^{-\partial_{\bar{x}}}} \bar{u} \Big|_{x_n}. \quad (41)$$

Using Eq. (41) in the pseudodifferential discrete governing Eq. (25), we get

$$D_1 \bar{u} + \alpha D_2 \bar{u} = D_3 \partial_{\bar{t}} \bar{u}, \quad (42)$$

where

$$D_1 = \frac{2(e^{\partial_{\bar{x}}} + e^{-\partial_{\bar{x}}} - 2)}{e^{\partial_{\bar{x}}} - e^{-\partial_{\bar{x}}}} \partial_{\bar{x}}, \quad (43)$$

$$D_2 = \frac{2(e^{2\partial_{\bar{x}}} + e^{-2\partial_{\bar{x}}} - 2)}{e^{\partial_{\bar{x}}} - e^{-\partial_{\bar{x}}}} \partial_{\bar{x}}, \quad (44)$$

$$D_3 = \frac{2}{e^{\partial_{\bar{x}}} - e^{-\partial_{\bar{x}}}} \partial_{\bar{x}}. \quad (45)$$

The previous expressions can be expanded by Taylor's series as

$$D_1 = \partial_{\bar{x}}^2 + \frac{1}{12} \partial_{\bar{x}}^4 + O(\partial_{\bar{x}}^6), \quad (46)$$

$$D_2 = \partial_{\bar{x}}^2 + \frac{1}{12} \partial_{\bar{x}}^4 + O(\partial_{\bar{x}}^6), \quad (47)$$

$$D_3 = 1 - \frac{1}{6} \partial_{\bar{x}}^2 + \frac{7}{360} \partial_{\bar{x}}^4 + O(\partial_{\bar{x}}^6). \quad (48)$$

Disregarding terms higher than second order, the governing equation takes the form

$$a_1 \partial_{\bar{x}\bar{x}} \bar{u} = \partial_{\bar{t}\bar{t}} \bar{u} - a_3 \partial_{\bar{x}\bar{x}\bar{t}\bar{t}} \bar{u}, \quad (49)$$

where

$$a_1 = 1 + 4\alpha; \quad a_3 = \frac{1}{6}. \quad (50)$$

This governing equation is similar to that of the EKE model (Eq. 38), with a different value of the parameter a_3 .

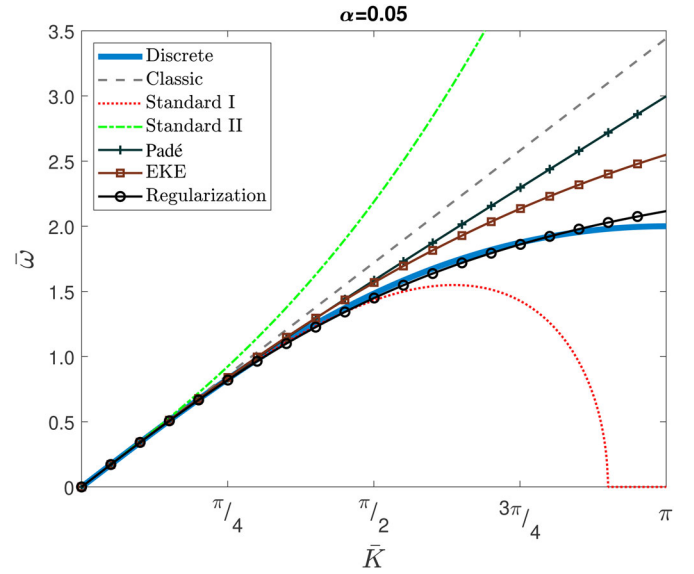


Figure 5. Dispersion curves for $\alpha = 0.05$. Comparison of the continuous models with the discrete model.

To finish this chapter, and with the intention of sum up the results achieved and compare the obtained governing and dispersion equations, the following general expressions are employed

$$a_1 \partial_{\bar{x}\bar{x}} \bar{u} - a_2 \partial_{\bar{x}\bar{x}\bar{x}\bar{x}} \bar{u} = \partial_{\bar{t}\bar{t}} \bar{u} - a_3 \partial_{\bar{x}\bar{x}\bar{t}\bar{t}} \bar{u}, \quad (51)$$

$$\bar{\omega} = \bar{K} \sqrt{\frac{a_1 + a_2 \bar{K}^2}{1 + a_3 \bar{K}^2}}, \quad (52)$$

which depend on the parameters a_1 , a_2 , and a_3 , shown for each model in Table 1.

4. Discussion

In this section, the dispersive curves obtained with the different studied models are compared to that derived from the discrete one, considered as reference. The same comparison is also provided for the phase velocity.

The different dispersion curves are shown in Figures 5 and 6. Each figure is devoted to a different value of the dimensionless parameter α (0.05 and 0.15, respectively).

As can be observed, all the models developed permit to reproduce the long wavelength propagation, since the dispersion curves match perfectly with that of the discrete system for low wavenumbers. However, this does not occur when the wavenumber increases. In this case, the behavior of the different models is analyzed in detail below.

Regardless of the reliability of the different models in capturing the dispersive behavior, it is necessary to point out several features of the different approaches. The Standard I model, has a major drawback since the propagation for wavenumbers $\bar{K} > \sqrt{12/(1 + 16\alpha)}$ is not stable. In such a case, imaginary frequencies appear, thus short waves grow exponentially in time without any external energy source, which is not consistent in a conservative system. This shortcoming, widely discussed in Metrikine and Askes [36] and Gazis and Wallis [14], does not appear in the other

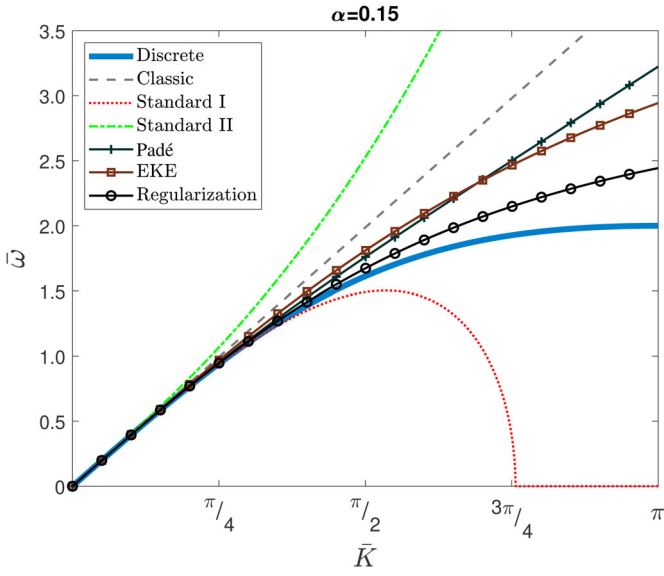


Figure 6. Dispersion curves for $\alpha = 0.15$. Comparison of the continuous models with the discrete model.

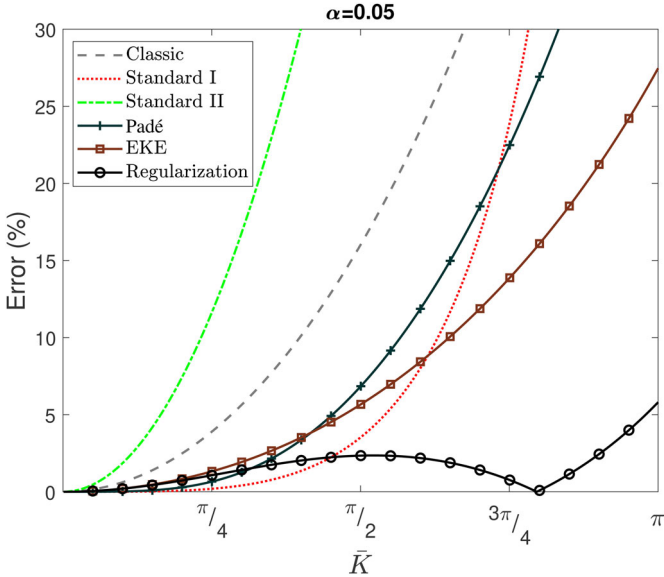


Figure 7. Relative error of the dispersion curves for $\alpha = 0.05$. Comparison of the continuous models with the discrete model.

studied models where the wave frequency presents real values for any wavenumber.

Another commonly studied feature is whether the group velocity is bounded from above, i.e., whether there is a maximum speed at which disturbances may propagate (see [36]). In the case of Standard II model, the group velocity is unbounded for any value of α , since it tends to infinity in the short wavelength limit. When using nonstandard continualization procedures, described in Section 3.2, this does not occur. The three of them lead to governing equations including an inertia length scale parameter a_3 which increases the flexibility of the model. Then, the group velocity tends to a constant value in the short wavelength limit.

Regarding the ability of the different models to reproduce the dispersion relation of the discrete system, Figures 7 and 8 show, for three different values of the dimensionless parameter α , the relative error defined as

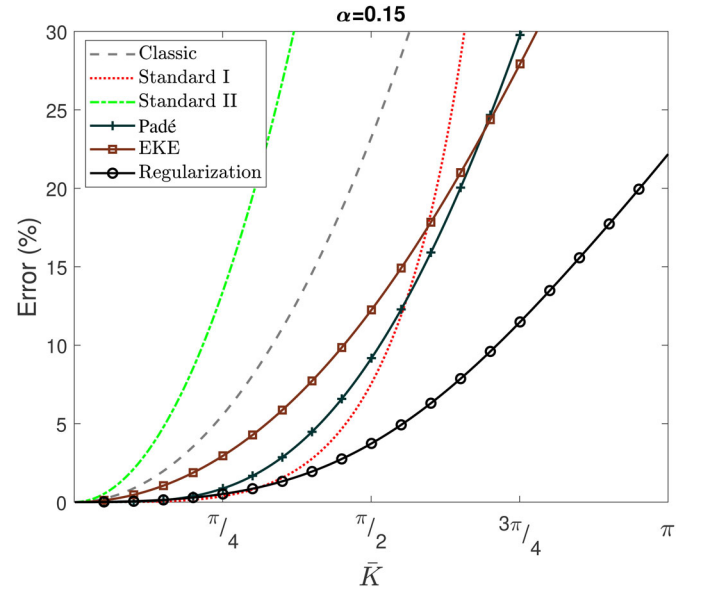


Figure 8. Relative error of the dispersion curves for $\alpha = 0.15$. Comparison of the continuous models with the discrete model.

$$\varepsilon(\%) = \frac{|\bar{\omega}_{\text{continuous}} - \bar{\omega}_{\text{discrete}}|}{\bar{\omega}_{\text{discrete}}} \times 100. \quad (53)$$

For long wavelengths, all continuous models present a small error, with Standard I, Padé, and Regularization models showing the best approximation. For small wavelengths, the equation obtained with the Regularization method clearly presents the lowest errors, close to 5% in the limit of the Brillouin zone ($\bar{K} = \pi$) for $\alpha = 0.05$, and around 22% in the case of $\alpha = 0.15$.

The comparison of the phase velocities derived from the different models shows similar results. Figures 9 and 10 present the variation of \bar{v}_{phase} for two different values of α . As it can be seen, the continuous model obtained with the regularization technique provides the best approximation to the discrete system.

Therefore, taking into account the physical consistency of the Regularization approach and the good approximation of the dispersion curve of the discrete system, this technique can be considered as a suitable method to describe with a continuous model the wave propagation through 1D linear lattice with nearest and next-nearest interactions. Furthermore, the governing equation achieved through this technique does not require nonclassical boundary condition to solve problems involving finite solids, widely used in engineering applications. Some examples of these applications are nanoelectromechanical and microelectromechanical sensors used in the field of biomedicine and biotechnology [29, 30], as well as in robotics and machines with significant weight or size problems [24, 25]. Another relevant problem where the inner structure of the solid is revealed in its dynamic properties can be found in the field of metamaterials, employed to control, and manipulate the wave propagation [26–28].

5. Conclusions

A large number of works deal with lattices with nearest neighbor interactions (Born Von-Kármán model), applying

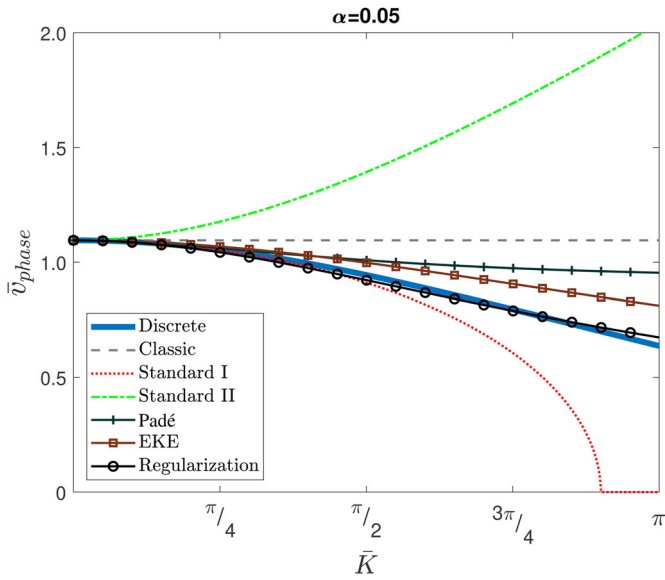


Figure 9. Phase velocity curves for $\alpha = 0.05$. Comparison of the continuous models with the discrete model.

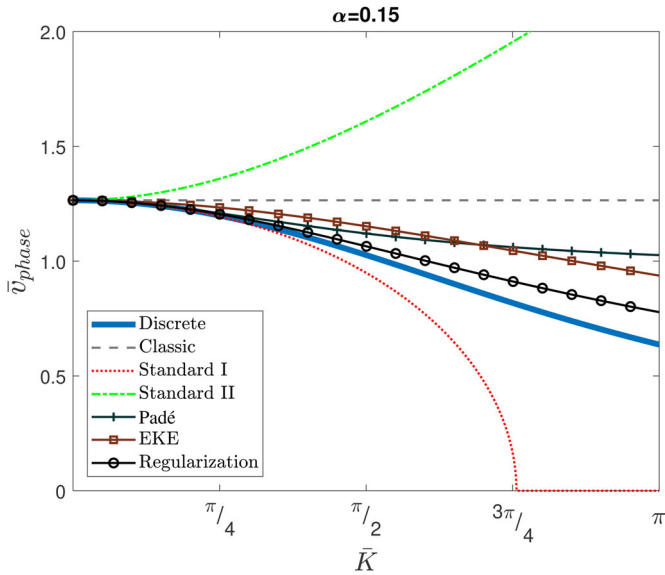


Figure 10. Phase velocity curves for $\alpha = 0.15$. Comparison of the continuous models with the discrete model.

different continualization methods. However, fewer frameworks study nearest and next-nearest neighbor interactions. In this article, a 1D linear lattice with nearest and next-nearest neighbor interactions has been continualized by different standard methods, as well as nonstandard techniques.

The main objective of this work is to compare the performance of all the models achieved by the different continualization techniques. To that aim, a benchmark test for the dispersion and phase velocity curves of the continuous governing equations have been realized. An analysis of the ability of these models to capture the dispersive behavior of the discrete system permitted to extract the following conclusions:

- If terms higher than second order are disregarded, all continualized models lead to the classical rod equation.

- When Standard I and II methods are applied, the continuous governing equations achieved have a fourth-order spatial derivative, thus nonclassical boundary conditions are needed. These boundary conditions can be derived from energy principles, but their physical meaning is unclear.
- The Standard I method leads to a model presenting physical inconsistencies. Its dispersion curve, although fits quite well that of the discrete system in the long-wavelength regime, has imaginary frequencies at short waves. Furthermore, this model is derived from a non-positive definite strain energy function; thus, the application of this model has to be prevented. Using the Standard II method, the elastic potential energy density is positive definite, but its group velocity is unbounded when the wavenumber tends to infinity.
- In Nonstandard methods, the drawbacks explained in the previous point are eliminated. However, the Padé model needs nonclassical boundary conditions when a finite (bounded) solid is studied. This does not occur with the governing equation obtained via both EKE and Regularization models.
- Applying the Padé method [8], to the lattice here studied, a fourth-order spatial derivative appears. However, by means of the EKE method, applied to the nearest and next-nearest interactions lattice the first time in this work, the fourth-order spatial derivative does not appear, and the structure of the continuous governing equation achieved is like the obtained in [8] (nearest interaction lattice), but including the influence of the parameter α .
- The Regularization method shows the best performance. Moreover, the governing equation achieved via this method does not lose the physical consistency nor needs nonclassical boundary conditions in bounded problems. The continuous governing equation has the same structure as that of the EKE model. However, the different coefficient in the term with spatial and time derivative leads to a better approximation to the dispersive behavior of the discrete system.

Nomenclature

\bar{x}_n	discrete dimensionless position
\bar{x}	continuous dimensionless position
\bar{t}	dimensionless time variable
\bar{u}_n	discrete dimensionless displacement
\bar{u}	continuous dimensionless displacement
$\bar{\omega}$	dimensionless wave frequency
\bar{K}	dimensionless wavenumber
$\bar{\mathcal{L}}$	dimensionless Lagrangian
$\bar{\mathcal{L}}_l$	dimensionless Lagrangian per unit of length
\bar{T}	dimensionless kinetic energy
\bar{T}_l	dimensionless kinetic energy per unit of length
\bar{W}	dimensionless potential energy
\bar{W}_l	dimensionless potential energy per unit of length
\bar{v}_{phase}	dimensionless phase velocity
$\partial_{\bar{x}}$	dimensionless spatial derivative
$\partial_{\bar{t}}$	dimensionless time derivative
k_1	stiffness of the interaction between nearest neighbors
k_2	stiffness of the interaction between next-nearest neighbors
α	interaction stiffness ratio

Declaration of interest statement

The authors declare that they have no known competing financial interests or personal relationships that could have appeared to influence the work reported in this paper.

Dedication

This work is dedicated to our dear friend and colleague Professor José Fernández-Sáez (University Carlos III de Madrid, Spain), a great scholar of Continuum and Structural Mechanics, in memory of his lively intelligence and scientific curiosity.

Funding

The authors wish to acknowledge the Ministerio de Economía y Competitividad de España for the financial support [Grant no. PGC2018-098218-B-I00].

References

- [1] Y. Tadi Beni, F. Mehralian, and H. Zeighampour, The modified couple stress functionally graded cylindrical thin shell formulation, *Mech. Adv. Mater. Struct.*, vol. 23, no. 7, pp. 791–801, 2016. DOI: [10.1080/15376494.2015.1029167](https://doi.org/10.1080/15376494.2015.1029167).
- [2] N. Shafiei, M. Kazemi, and L. Fatahi, Transverse vibration of rotary tapered microbeam based on modified couple stress theory and generalized differential quadrature element method, *Mech. Adv. Mater. Struct.*, vol. 24, no. 3, pp. 240–252, 2017. DOI: [10.1080/15376494.2015.1128025](https://doi.org/10.1080/15376494.2015.1128025).
- [3] R. Barretta, S. A. Faghidian, and R. Luciano, Longitudinal vibrations of nano-rods by stress-driven integral elasticity, *Mech. Adv. Mater. Struct.*, vol. 26, no. 15, pp. 1307–1315, 2019. DOI: [10.1080/15376494.2018.1432806](https://doi.org/10.1080/15376494.2018.1432806).
- [4] D. Polyzos and D. Fotiadis, Derivation of Mindlin's first and second strain gradient elastic theory via simple lattice and continuum models, *Int. J. Solids Struct.*, vol. 49, no. 3–4, pp. 470–480, 2012. DOI: [10.1016/j.ijsolstr.2011.10.021](https://doi.org/10.1016/j.ijsolstr.2011.10.021).
- [5] R. D. Mindlin, *Microstructure in linear elasticity*, Tech. Rep., Columbia University, New York, 1963.
- [6] I. V. Andrianov, G. A. Starushenko, and D. Weichert, Numerical investigation of 1D continuum dynamical models of discrete chain, *Z. Angew. Math. Mech.*, vol. 92, no. 11–12, pp. 945–954, 2012. DOI: [10.1002/zamm.201200057](https://doi.org/10.1002/zamm.201200057).
- [7] A. Bacigalupo and L. Gambarotta, Generalized micropolar continualization of 1D beam lattices, *Int. J. Mech. Sci.*, vol. 155, pp. 554–570, 2019. DOI: [10.1016/j.ijmecsci.2019.02.018](https://doi.org/10.1016/j.ijmecsci.2019.02.018).
- [8] P. Kevrekidis, I. Kevrekidis, A. Bishop, and E. Titi, Continuum approach to discreteness, *Phys. Rev. E*, vol. 65, no. 4, pp. 046613, 2002. DOI: [10.1103/PhysRevE.65.046613](https://doi.org/10.1103/PhysRevE.65.046613).
- [9] P. Rosenau, Hamiltonian dynamics of dense chains and lattices: Or how to correct the continuum, *Phys. Lett. A*, vol. 311, no. 1, pp. 39–52, 2003. DOI: [10.1016/S0375-9601\(03\)00455-9](https://doi.org/10.1016/S0375-9601(03)00455-9).
- [10] J. Vila, J. Fernández-Sáez, and R. Zaera, Nonlinear continuum models for the dynamic behavior of 1D microstructured solids, *Int. J. Solids Struct.*, vol. 117, pp. 111–122, 2017. DOI: [10.1016/j.ijsolstr.2017.03.033](https://doi.org/10.1016/j.ijsolstr.2017.03.033).
- [11] E. Fermi, P. Pasta, S. Ulam, and M. Tsingou, *Studies of the nonlinear problems*, Tech. Rep., Los Alamos Scientific Laboratory, New Mexico, 1955.
- [12] N. Challamel, H. Zhang, C. Wang, and J. Kaplunov, Scale effect and higher-order boundary conditions for generalized lattices, with direct and indirect interactions, *Mech. Res. Commun.*, vol. 97, pp. 1–7, 2019. DOI: [10.1016/j.mechrescom.2019.04.002](https://doi.org/10.1016/j.mechrescom.2019.04.002).
- [13] F. Y. Chen, On modeling and direct solution of certain free vibration systems, *J. Sound Vib.*, vol. 14, no. 1, pp. 57–79, 1971. DOI: [10.1016/0022-460X\(71\)90507-4](https://doi.org/10.1016/0022-460X(71)90507-4).
- [14] D. Gazis and R. Wallis, Surface tension and surface modes in semi-infinite lattices, *Surf. Sci.*, vol. 3, no. 1, pp. 19–32, 1965. DOI: [10.1016/0039-6028\(65\)90015-4](https://doi.org/10.1016/0039-6028(65)90015-4).
- [15] R. D. Mindlin, Second gradient of strain and surface-tension in linear elasticity, *Int. J. Solids Struct.*, vol. 1, pp. 417–438, 1965.
- [16] H. Eaton and J. Peddieson Jr, On continuum description of one-dimensional lattice mechanics, *J. Tenn. Acad. Sci.*, vol. 48, pp. 96–100, 1973.
- [17] G. A. Maugin, *Nonlinear Waves in Elastic Crystals*, Oxford University Press, Oxford, 1999.
- [18] N. Triantafyllidis and S. Bardenhagen, On higher order gradient continuum theories in 1-D nonlinear elasticity. Derivation from and comparison to the corresponding discrete models, *J. Elasticity*, vol. 33, no. 3, pp. 259–293, 1993. DOI: [10.1007/BF00043251](https://doi.org/10.1007/BF00043251).
- [19] A. Metrikine, On causality of the gradient elasticity models, *J. Sound Vib.*, vol. 297, no. 3–5, pp. 727–742, 2006. DOI: [10.1016/j.jsv.2006.04.017](https://doi.org/10.1016/j.jsv.2006.04.017).
- [20] M. Di Paola, A. Pirrotta, and M. Zingales, Mechanically-based approach to nonlocal elasticity: Variational principles, *Int. J. Solids Struct.*, vol. 47, no. 5, pp. 539–548, 2010. DOI: [10.1016/j.ijsolstr.2009.09.029](https://doi.org/10.1016/j.ijsolstr.2009.09.029).
- [21] M. Zingales, Wave propagation in 1D elastic solids in presence of long-range central interactions, *J. Sound Vib.*, vol. 330, no. 16, pp. 3973–3989, 2011. DOI: [10.1016/j.jsv.2010.10.027](https://doi.org/10.1016/j.jsv.2010.10.027).
- [22] V. E. Tarasov, Lattice model with nearest-neighbor and next-nearest-neighbor interactions for gradient elasticity, *Interdiscip J DNC*, vol. 4, no. 1, pp. 11–23, 2015. DOI: [10.5890/DNC.2015.03.002](https://doi.org/10.5890/DNC.2015.03.002).
- [23] C. R. Martin, Membrane-based synthesis of nanomaterials, *Chem. Mater.*, vol. 8, no. 8, pp. 1739–1746, 1996. DOI: [10.1021/cm960166s](https://doi.org/10.1021/cm960166s).
- [24] T. Braun, V. Barwich, M. K. Ghatkesar, A. H. Bredekamp, C. Gerber, M. Hegner, and H. P. Lang, Micromechanical mass sensors for biomolecular detection in a physiological environment, *Phys. Rev. E*, vol. 72, no. 3, pp. 031907, 2005. DOI: [10.1103/PhysRevE.72.031907](https://doi.org/10.1103/PhysRevE.72.031907).
- [25] K. Eom, H. S. Park, D. S. Yoon, and T. Kwon, Nanomechanical resonators and their applications in biological/chemical detection: Nanomechanics principles, *Phys. Rep.*, vol. 503, no. 4–5, pp. 115–163, 2011. DOI: [10.1016/j.physrep.2011.03.002](https://doi.org/10.1016/j.physrep.2011.03.002).
- [26] N. Kundtz and D. R. Smith, Extreme-angle broadband metamaterial lens, *Nat. Mater.*, vol. 9, no. 2, pp. 129–132, 2010. DOI: [10.1038/nmat2610](https://doi.org/10.1038/nmat2610).
- [27] D. Lee, D. M. Nguyen, and J. Rho, Acoustic wave science realized by metamaterials, *Nano Converg.*, vol. 4, no. 1, pp. 3, 2017. DOI: [10.1186/s40580-017-0097-y](https://doi.org/10.1186/s40580-017-0097-y).
- [28] Y. L. Loo, Y. Yang, N. Wang, Y. G. Ma, and C. K. Ong, Broadband microwave Luneburg lens made of gradient index metamaterials, *J. Opt. Soc. Am. A Opt. Image Sci. Vis.*, vol. 29, no. 4, pp. 426–430, 2012. DOI: [10.1364/JOSAA.29.000426](https://doi.org/10.1364/JOSAA.29.000426).
- [29] H. S. Hosseini, M. Horáák, P. K. Zysset, and M. Jirásek, An over-nonlocal implicit gradient-enhanced damage-plastic model for trabecular bone under large compressive strains, *Int. J. Numer. Methods Biomed. Eng.*, vol. 31, no. 11, e02728, 2015. DOI: [10.1002/cnm.2728](https://doi.org/10.1002/cnm.2728).
- [30] A. Madeo, D. George, T. Lekszycki, M. Nierenberger, and Y. Rémond, A second gradient continuum model accounting for some effects of micro-structure on reconstructed bone remodeling, *C. R. Mécanique*, vol. 340, no. 8, pp. 575–589, 2012. DOI: [10.1016/j.crme.2012.05.003](https://doi.org/10.1016/j.crme.2012.05.003).
- [31] L. Brillouin, *Wave Propagation in Periodic Structures: Electric Filters and Crystal Lattices*, McGraw-Hill Book Company, New York, 1946.
- [32] A. C. Eringen, Linear theory of nonlocal elasticity and dispersion of plane waves, *Int. J. Eng. Sci.*, vol. 10, no. 5, pp. 425–435, 1972. DOI: [10.1016/0020-7225\(72\)90050-X](https://doi.org/10.1016/0020-7225(72)90050-X).

- [33] D. De Domenico, H. Askes, and E. C. Aifantis, Discussion of “Derivation of Mindlin’s first and second strain gradient elastic theory via simple lattice and continuum models” by Polyzos and Fotiadis, *Int. J. Solids Struct.*, vol. 191–192, pp. 646–651, 2020. DOI: [10.1016/j.ijsolstr.2019.11.016](https://doi.org/10.1016/j.ijsolstr.2019.11.016).
- [34] D. Polyzos and D. Fotiadis, Reply to “Discussion of “Derivation of Mindlin’s first and second strain gradient elastic theory via simple lattice and continuum models” by Polyzos and Fotiadis, *Int. J. Solids Struct.*, vol. 191–192, pp. 652–654, 2020. DOI: [10.1016/j.ijsolstr.2019.11.017](https://doi.org/10.1016/j.ijsolstr.2019.11.017).
- [35] N. Challamel, Z. Zhang, C. M. Wang, J. N. Reddy, Q. Wang, T. Michelitsch, and B. Collet, On nonconservativeness of Eringen’s nonlocal elasticity in beam mechanics: Correction from a discrete-based approach, *Arch. Appl. Mech.*, vol. 84, no. 9–11, pp. 1275–1292, 2014. DOI: [10.1007/s00419-014-0862-x](https://doi.org/10.1007/s00419-014-0862-x).
- [36] A. V. Metrikine and H. Askes, One-dimensional dynamically consistent gradient elasticity models derived from a discrete microstructure: Part 1: Generic formulation, *Eur. J. Mech. A Solids*, vol. 21, no. 4, pp. 555–572, 2002. DOI: [10.1016/S0997-7538\(02\)01218-4](https://doi.org/10.1016/S0997-7538(02)01218-4).

Appendix: Disregarding high-order terms in the Padé model

In Eq. (29), terms higher of third order in l^3 are dismissed. If this equation is rewritten in dimensional form

$$\begin{aligned} & l^2(k_1 + 4k_2)\partial_{xx}u - \frac{1}{3}l^4(k_1 + k_2)\partial_{xxxx}u \\ &= \frac{1}{\tilde{\omega}^2}\partial_{tt}u - \frac{5}{15}\frac{l^2}{\tilde{\omega}^2}\partial_{xxtt}u + \frac{1}{36}\frac{l^4}{\tilde{\omega}^2}\partial_{xxxxtt}u, \end{aligned} \quad (\text{A1})$$

and taking into account that

$$\tilde{\omega}^2 = \frac{k_1}{M} = \frac{k_1}{\rho l}, \quad (\text{A2})$$

$$\begin{aligned} & l(k_1 + 4k_2)\partial_{xx}u - \frac{1}{3}l^3(k_1 + k_2)\partial_{xxxx}u \\ &= \frac{\rho}{k_1}\partial_{tt}u - \frac{5}{15}\frac{\rho l^2}{k_1}\partial_{xxtt}u + \frac{1}{36}\frac{\rho l^4}{k_1}\partial_{xxxxtt}u, \end{aligned} \quad (\text{A3})$$

it can be checked that there is a derivative multiplied by l^4 (term smaller than the rest) which can be disregarded.